Published in final edited form as:
Invest New Drugs. 2011 October ; 29(5): 901–911. doi:10.1007/s10637-010-9445-z.

Pharmacokinetics and derivation of an anticancer dosing regimen for PAC-1 in healthy dogs

Pamela W. Lucas, **Joanna M. Schmit**, **Quinn P. Peterson**, **Diana C. West**, **Danny C. Hsu**, **Chris J. Novotny**, **Levent Dirikolu**, **Daniel R. Deorge**, **Laura D. Garrett**, **Paul J. Hergenrother**, and **Timothy M. Fan**

Comparative Oncology Research Laboratory, Department of Veterinary Clinical Medicine, University of Illinois at Urbana-Champaign: (TMF, PWL, JMS, and LDG), Division of Biochemical Toxicology, National Center for Toxicological Research, U.S. Food and Drug Administration: (DRD), Department of Chemistry, University of Illinois at Urbana-Champaign: (DCW, DCH, and PJH), Department of Biochemistry, University of Illinois at Urbana-Champaign (QPP, CJN, and PJH), Department of Veterinary Bioscience, University of Illinois at Urbana-Champaign: (LD)

Abstract

PAC-1 is a preferential small molecule activator of procaspase-3 and has potential to become a novel and effective anticancer agent. The rational development of PAC-1 for translational oncologic applications would be advanced by coupling relevant *in vitro* cytotoxicity studies with pharmacokinetic investigations conducted in large mammalian models possessing similar metabolism and physiology as people. In the present study, we investigated whether concentrations and exposure durations of PAC-1 that induce cytotoxicity in lymphoma cell lines *in vitro* can be achievable in healthy dogs through a constant rate infusion (CRI) intravenous delivery strategy. Time- and dose-dependent procaspase-3 activation by PAC-1 with subsequent cytotoxicity was determined in a panel of B-cell lymphoma cells *in vitro*. The pharmacokinetics of PAC-1 administered orally or intravenously was studied in 6 healthy dogs using a crossover design. The feasibility of maintaining steady state plasma concentration of PAC-1 for 24 or 48 hours that paralleled *in vitro* cytotoxic concentrations was investigated in 4 healthy dogs. *In vitro,* PAC-1 induced apoptosis in lymphoma cell lines in a time- and dose-dependent manner. The oral bioavailability of PAC-1 was relatively low and highly variable (17.8 ± 9.5%). The achievement and maintenance of predicted PAC-1 cytotoxic concentrations in normal dogs was safely attained via intravenous CRI lasting for 24 or 48 hours in duration. Using the dog as a large mammalian model, PAC-1 can be safely administered as an intravenous CRI while achieving predicted *in vitro* cytotoxic concentrations.

Apoptosis or programmed cell death is a normal and controlled end to cellular life, and is characterized by cellular changes including nuclear pyknosis, chromatin condensation, membrane blebbing, cytoskeletal collapse, and formation of apoptotic bodies (Li and Yuan, 2008). Appropriate programmed cell death is necessary for maintaining cellular homeostasis (e.g. lymphocyte apoptosis), and also regulates anatomic development of various organs and soft tissues (Mori et al., 1995; Takanosu et al., 2002). The preservation of normal apoptotic signals is necessary for maintaining genomic integrity of host organisms, which thwarts the successful replication of somatic cells harboring mutated or damaged DNA, so as to prevent malignant transformation (Medema and Borst, 1999; Hildeman et al., 2002; Arnold et al., 2006).

Timothy M. Fan, DVM, PhD, Department of Veterinary Clinical Medicine, University of Illinois at Urbana-Champaign, Urbana, Illinois 61802-4714, Tel: (217) 333-5375, t-fan@illinois.edu.

The evasion of normal death signals is one of the major changes leading to tumor formation (Hanahan and Weinberg, 2000). Frequently described defects in the apoptotic machinery of cancer cells include mutations in tumor suppressor genes, p53 and PTEN, and overexpression of antiapoptotic proteins such as bcl-2 (Gurumurthy et al., 2001; Downward, 2004). Mechanistically, programmed cell death is a coordinated process that requires the controlled and serial activation of key proteases characterized as cysteine aspartases, called caspases. Apoptotic caspases can be segregated based upon their protein structure into either initiator caspases (caspase-2, -8, -9, -10, -12) or executioner caspases (caspase-3, -6, -7) (Li and Yuan, 2008). Maintained as preformed, low-activity zymogens (procaspases) in the cytosol, the proteolytic activities of caspases are tightly regulated, and only induced following key cellular signals mediated by extrinsic and intrinsic events (Pop and Salvesen, 2009). Putatively, the activation of procaspase-3 to caspase-3 is a pivotal and committed step for programmed cell death, given the multitude of substrates that are cleaved by caspase-3, as well as its most downstream position in the apoptotic cascade (Li and Yuan, 2008). Given the key role of active caspase-3 for apoptosis, it is not surprising that many solid tumors and hematopoietic cancers in people preferentially inhibit the autocatalytic conversion of procaspase-3 to caspase-3, and thereby shift the balance towards resistance of programmed cell death (Nakagawara et al., 1997; Izban et al., 1999; Fink et al., 2001; O'Donovan et al., 2003; Krepela et al., 2004).

In 2006, a small molecule called PAC-1 was identified as the first procaspase activating compound which demonstrated promising anticancer properties both *in vitro* and in mouse xenograft models (Putt et al., 2006). Mechanistically, PAC-1 induces apoptotic death in cancer cells through the chelation of inhibitory zinc from procaspase-3, allowing for its autocatalytic activation and subsequent generation of caspase-3 (Peterson et al., 2009a; Peterson et al., 2009b). As the first procaspase-activating compound, further experiments with PAC-1 can begin to define the potential of procaspase-3 activation as a viable anticancer strategy for human patients. Of the various lethal tumor histologies diagnosed in people, Non-Hodgkin's lymphoma may be a relevant model for evaluating PAC-1. Given that variants of Non-Hodgkin's lymphoma possess high concentrations of procaspase-3 and cure rates for specific lymphoma subtypes remains relatively low (40–50%), evaluating PAC-1 as a novel therapeutic for lymphoma appears mechanistically and clinically warranted (Fisher et al., 1993; Dukers et al., 2002; Muris et al., 2005).

To further develop PAC-1 as an experimental therapeutic for the treatment of Non-Hodgkin's lymphoma in humans, specifically diffuse large B-cell lymphoma, we first sought to identify the *in vitro* conditions by which PAC-1 induces caspase-3 activity and exerts cytotoxic effects against a panel of immortalized B-cell lymphoma lines. Second, we characterized the pharmacokinetics of intravenous and oral PAC-1 in a large mammalian model, the dog, which closely resembles the physiology and metabolism of human beings. Last, we assessed the feasibility and safety of a pharmacokinetically-derived dosing regimen which achieved and maintained steady-state concentrations of PAC-1 in dogs predicted to correlate with *in vitro* cytotoxic concentrations.

MATERIALS AND METHODS

Cell lines and reagents

Two canine B-cell lymphoma lines (17-71 and GL-1) were provided by Dr. Steve Suter, North Carolina State University. These cells were maintained in Dulbecco's Modified Eagle's Medium (DMEM) supplemented with 10% fetal bovine serum (FBS), penicillin and streptomycin (P/S). A human B-cell lymphoma line, CA46, was purchased from American Tissue Culture Collection (Manassas, VA) and maintained in DMEM supplemented with 20% FBS and P/S. All three lymphoma cell lines grew as free suspensions in cell culture

flasks (Corning, Inc., Corning, NY) when incubated at 37 °C in 5% CO_2, and cultures were passaged 2–3 times a week to maintain high cell viability. As necessary, cells were harvested and a trypan blue dye exclusion test was performed to assess viability ≥ 95% prior to any experimentation.

PAC-1 and deuterated PAC-1 were synthesized as described (Putt et al., 2006). For all *in vitro* experiments, PAC-1 was reconstituted with 99.5% DMSO (Sigma-Aldrich, St. Louis, MO) to produce a 10 mM stock solution, which then was aliquoted and kept frozen at −20°C until needed. For all *in vivo* experiments, PAC-1 was freshly reconstituted to a concentration of 15 mg/ml immediately prior to infusion by solubilizing in 2-hydoxypropyl-β-cyclodextrin (Sigma-Aldrich, St. Louis, MO) and sterile water for injection.

In vitro procaspase-3 analysis

To demonstrate the cellular target of PAC-1, endogenous procaspase-3 was assessed in all three B-cell lymphoma lines. One million cells each of 17-71, GL-1, and CA46 cells were harvested, washed in phosphate buffered saline (PBS), resuspended in 1 ml of fixation/permeabilization working solution (eBioscience, San Diego, CA), and incubated on ice for 2 hours. Following fixation and permeabilization, cells were washed twice with permeabilization buffer, and then incubated either with rabbit anti-mouse procaspase-3 antibody (1:25, Epitomics, Burlingame, CA) or rabbit IgG isotype control antibody (1:25, SCB, Santa Cruz, CA), incubated at 4 °C overnight, and then washed once with permeabilization buffer. Cells were incubated with secondary sheep anti-rabbit IgG:RPE (1:10, AbD Serotec, Raleigh, NC) at 4 °C in the dark for 60 minutes, washed twice in permeabilization buffer and analyzed by flow cytometry (Beckman Coulter Epics XL).

In vitro PAC-1 cytotoxicity studies

Fresh media containing varying concentrations of PAC-1 (0, 5, 10, and 20 μM) were added to a 6-well plate containing 100,000 cells/well for either 24 or 48 hours at 37 °C in 5% CO_2. All lymphoma cell lines, 17-71, GL-1, and CA46, were evaluated and all experiments were performed in triplicate. For analysis of cytotoxicity, an Annexin V-FITC/PI apoptosis detection kit (BD Pharmingen, San Diego, CA) was used according to the manufacturer's directions and analyzed by flow cytometry (Beckman Coulter Epics XL).

In vitro caspase-3 activation

Caspase-3 activation was assessed by exposing lymphoma cells to 10 or 20 μM of PAC-1 for 0, 1, 2, 4, 24, and 48 hours at 37 °C in 5% CO_2. Caspase-3 activity produced by 2 million cells per time point were analyzed and experiments were performed in duplicate. Caspase-3 activity was quantified in cell lysate using a commercially-available caspase-3 colorimetric assay (R & D Systems, Minneapolis, Minnesota), and reactions were read on a Bio-Tek EL-800 microplate reader using a 405nm wavelength. Relative caspase-3 activities were expressed and compared as optical density (OD) measurements.

Animals and sample collection

Six healthy, intact male hound dogs weighing at least 30 kg were used for all pharmacokinetic studies. All procedures involving care and handling of the dogs followed guidelines set forth by the University of Illinois Animal Care and Use Committee. Pharmacokinetic analyses were derived from PAC-1 dissolved in 2-hydoxypropyl-β-cyclodextrin and sterile water, and dosed at 1.0 mg/kg body weight as either a 10-minute intravenous (IV) bolus or 5-minute oral slurry. All dogs received a single dose of PAC-1 via both IV and oral routes, with a two-week washout period between dosing. Blood was drawn from the jugular vein, centrifuged, and plasma stored at −80°C until analysis. Sample

collection times for dogs receiving IV PAC-1 were 0, 10, 20, 30, 40, 60, 120, 240, 480, 720 minutes, and 24 hours post administration. Sample collection times for dogs administered oral PAC-1 were 0, 15, 30, 45, 60, 120, 240, 480, 720 minutes, and 24 hours post administration.

Pharmacokinetic-derived dosing regimen and toxicity assessment of constant rate infusion PAC-1

Following the pharmacokinetic characterization of IV PAC-1, a dosing regimen predicted to achieve and maintain a steady state plasma concentration of 10 μM or greater was derived and tested in 4 of the original 6 hound dogs. These 4 dogs were treated with IV PAC-1 delivered as a constant rate infusion (CRI), comprising of a 10-minute loading dose (LD), and followed by a constant maintenance dose (MD) for 48 hours. Blood samples were collected at 0, 1, 6, 12, 24, 36 and 48 hours to determine PAC-1 plasma concentrations. Following PAC-1 infusion, dogs were assessed for any potential hematologic, non-hematologic, or gastrointestinal side effects weekly for 4 consecutive weeks.

Liquid chromatography-Mass Spectrometry (LC/MS) Analysis of PAC-1

A Waters Alliance 2795 Separation Module (Waters Co., Milford, MA) was used at a flow rate of 200 ml/min to deliver an isocratic mobile phase consisting of 32% (v:v) acetonitrile in aqueous 0.1% formic acid (v:v). Separations were conducted using a Luna C18 (2) column (2 × 150 mm, 3 μ particle size (Phenomenex, Torrance CA) maintained at ambient temperature. An AD20 detector (Dionex Co., Sunnyvale, CA) was used to assess chemical purity and to quantify the internal standard (254 nm detection).

A Micromass Quattro Ultima (Waters Co.) triple quadrupole mass spectrometer equipped with an electrospray probe was used in multiple reactions monitoring (MRM) mode for analysis of positive ions. The optimal MRM transitions (*i.e*., those giving the maximal responses) for PAC-1 and deuterated PAC-1 were determined to be *m/z* 393 -->189 and 400 -->196, respectively (*i.e*., $[M+H]^+$ -->benzyl-piperazine=CH_2^+). Other MS parameters included dwell times of 0.2 sec, argon collision gas at 2.2×10^{-3} bar, nitrogen as both cone gas (100 L/hr) and desolvation gas (750 L/hr), and source and desolvation temperatures of 100 °C and 350 °C, respectively. An optimized sampling cone-skimmer potential of 50 V and a collision energy of 25 eV were used was used throughout. Resolution was set to give peak widths at half-height of 0.9 Th for product and precursor ions.

Characterization of labeled internal standard

The solution concentration of deuterated PAC-1 was determined by comparing LC-UV response (254 nm) with that from a solution of the authentic unlabeled analog prepared by accurate weighing. No unlabeled PAC-1 was observed using full scan MS or MRM monitoring (<0.1%). The plot of response ratios for labeled versus unlabeled PAC-1 was linear over the concentration range of 2.5–250 fmol unlabeled plus 100 fmol deuterated PAC-1 with a slope of 0.97 and a correlation coefficient of 0.999. Seven different concentration ratios, analyzed in duplicate, were used for the plot and all back-calculated concentrations were within 10% of the nominal value.

Solid phase extraction

Thawed serum samples (10 μl) and 100 fmol deuterated PAC-1 internal standards (in 10 μl acetonitrile) were added to a total of 500 μl of 50 mM ammonium acetate (pH 7.2). Solid phase extraction was performed in the 96-well format using an Oasis HLB plate (Waters Corp., 10 mg wells). The wells were activated by sequential application of 1 ml methanol and 1 ml 50 mM ammonium acetate (pH 7.2). The samples were applied and the cartridges

were washed with 0.5 ml of 50 mM ammonium acetate (pH 7.2) and then eluted with 2 × 0.5 ml methanol containing 0.1% formic acid (v/v). The samples were concentrated to approximately 30 ml using a centrifugal vacuum concentrator (SpeedVac, Savant, Farmingdale, NY) and 50 μl methanol containing 0.1% formic acid (v/v) and then 50 μl water were added. Aliquots of 10 ml were analyzed using LC-ES/MS/MS.

Pharmacokinetic determinations

Pharmacokinetic analyses were performed, using a non-linear regression program (Winnonlin, version 5.1) (Pharsight Corporation, Cary, NC). Area under the curve (AUC) following intravenous administration was measured by use of a linear trapezoidal approximation with extrapolation to infinity, and slope of the terminal portion (β) of the log plasma drug concentrations versus time curve was determined by the method of least-squares regression (Gibaldi and Perrier, 1982).

The compartmental model used is represented by general equation *a* where Cp is plasma concentration of compound at any time (t), A and B are the Y intercepts associated with distribution and elimination phase, respectively, and α and β represent the rate constant of distribution and terminal elimination phase, respectively. The rate constant of distribution (α), and distribution half-life ($t_{1/2}$ α) were determined using the method of residuals (Gibaldi and Perrier, 1975). The terminal half-life ($t_{1/2}$ β) (Martinez, 1998b; Martinez, 1998a) was calculated according to Equation 1.

$$Cp = A \times e^{-\alpha.t} + B \times e^{-\beta.t} \quad (a)$$

$$t_{1/2}\beta = \ln 2/\beta \quad (1)$$

Total body clearance (Cl_s) was calculated by use of Equation 2.

$$Cl_s = \text{IV Dose}/AUC_{0-inf}(IV). \quad (2)$$

The absolute bioavailability (F) was calculated from the $AUC_{0\text{-inf}}$ ratio obtained following oral and IV administration according to Equation 3.

$$F = AUC_{0-inf}(\text{Oral})/AUC_{0-inf}(IV) \times \text{IV Dose}/\text{Oral Dose} \quad (3)$$

The volume of distribution in central compartment (Vd_c), volume of distribution in terminal elimination phase (Vd_β) and volume of distribution at steady state (Vd_{ss}) were calculated according to Equations 4, 5 and 6, respectively (Martinez, 1998b; Martinez, 1998a).

$$Vd_c = \text{Dose}(IV)/A + B \quad (4)$$

$$Vd_\beta = \text{IV Dose}/AUC_{0-inf} \times \beta \quad (5)$$

$$Vd_{ss} = \text{IV Dose} \times AUMC_{0-inf}/(AUC_{0-inf})^2 \quad (6)$$

AUMC is area under the first moment curve and calculated by the trapezoidal method and extrapolated to infinity (Gibaldi and Perrier, 1982).

The compartmental model used following oral administration is represented by general equation *b* where A is Y intercept associated with terminal elimination phase, K_{01} is the apparent rate constant of absorption, and K_{10} is the apparent rate constant of elimination (Shargel, 1993). The rate constant of absorption (K_{01}) and the absorption half-life ($t_{1/2}$ K_{01}) were determined, using the method of residuals (Gibaldi and Perrier, 1975). The linear terminal slope (K_{10}) was calculated from the log plasma drug concentrations versus time curve by using the method of least-squares regression (Gibaldi and Perrier, 1982). The terminal elimination half-life ($t_{1/2}$ K_{10}) was calculated according to equation 7.

$$Cp = A \times e^{-K10.t} - A \times e^{-K01.t} \quad (b)$$

$$t_{1/2}K_{10} = \ln 2 / K_{10} \quad (7)$$

Total oral clearance (Cl_o) will be calculated by use of Equation 8

$$Cl_o = \text{Dose(Oral)} / AUC_{0-inf} \quad (8)$$

The maximum drug concentration after oral administration (C_{max}) and the time at which C_{max} was achieved (T_{max}) (Martinez, 1998b; Martinez, 1998a)were determined by use of equations 9 and 10, respectively.

$$C_{max} = A.e^{-K10.Tmax} - A.e^{-K01.Tmax} \quad (9)$$

$$T_{max} = 1/K_{01} - K_{10} \times (\text{Ln}(K_{01}/K_{10}) \quad (10)$$

Statistical analysis

The effect of two variables, being incubation time (time-dependent) and PAC-1 concentration (dose-dependent), on cytotoxicity in the 17-71, GL-1, and CA46 cell lines were compared with a 2-way ANOVA test. Significance was evaluated with either Tukey or Dunnett's post hoc tests for time-dependent or concentration-dependent variables, respectively. Differences in caspase-3 activation following incubation with PAC-1 (10 or 20 μM) for varying exposure durations were analyzed with one-way ANOVA and post-hoc Dunnett's test. Significance was defined as $p < 0.05$.

RESULTS

Procaspase-3 analysis

Compared with the staining intensity produced by the isotype control antibody, all three B-cell lymphoma lines, 17-71, GL-1, and CA46, expressed measurable procaspase-3 concentrations as detected by flow cytometry (Figure 1). Qualitative differences in procaspase-3 concentrations among cell lines were compared by their relative mean fluorescent intensity (MFI) ratios expressed as the fraction (procaspase-3 MFI)/(isotype control MFI). The relative concentration of procaspase-3 was greatest in the canine lymphoma cell line, 17-71, with a relative MFI ratio of 2.4, in comparison with ratios of 1.7

and 1.8 corresponding to GL-1 and CA46, respectively. Based upon a prior study where PAC-1 IC_{50} values correlated proportionally with procaspase-3 concentrations (Putt et al., 2006), it was expected that the 17-71 lymphoma cell line would be most sensitive to the apoptotic inducing effects of PAC-1.

In vitro conditions with PAC-1 apoptosis

We sought to characterize the minimal *in vitro* conditions by which PAC-1 could induce apoptosis in a time- and dose-dependent manner. For all cell lines, 17-71, GL-1, and CA46, variable degrees of cytotoxicity dictated by either PAC-1's exposure duration (24–48 hours) or concentration (5–20 μM) were identified. Furthermore, a significant and positive interaction between PAC-1's exposure duration (time-dependent) and concentration (dose-dependent) on cytotoxicity were identified for all three lymphoma cells lines, $p < 0.01$.

As expected by MFI ratios, 17-71 cells were more susceptible to the apoptotic inducing properties of PAC-1, as demonstrated by the detection of cells undergoing early apoptosis with PAC-1 concentrations of 10 μM or greater (Figure 2). Following 24 hours of drug exposure, PAC-1 increased the percentage of apoptotic cells modestly (~10–15%) above untreated or vehicle-treated cells in a dose-dependent fashion (Figure 3a). After 48 hours, the majority (≥ 60%) of 17-71 cells were apoptotic with PAC-1 concentrations ≥ 10 μM (Figure 3b). Another canine B-cell lymphoma line, GL-1, was less sensitive to the apoptotic inducing effects of PAC-1. Only marginal increases in the percentage of apoptotic cells (~10%) above untreated or vehicle control cells were detected following 24 hours of PAC-1 incubation at even the highest concentration of 20 μM (Figure 3c). Even following 48 hours, the majority (~ 60%) of GL-1 cells remained viable despite exposure to 20 μM of PAC-1 (Figure 3d). More similar to 17-71 cells, the human B-cell lymphoma line, CA46, was also relatively sensitive to PAC-1. Following a 24 hour exposure to PAC-1, a significant fraction (~20–35%) of cells was apoptotic (Figure 3e). With a PAC-1 incubation duration of 48 hours, greater than 50% of cells had undergone apoptosis with PAC-1 concentrations ≥10 μM (Figure 3f).

Caspase-3 activation studies

To more fully characterize the mechanism of cytotoxicity exerted by PAC-1 *in vitro*, we assessed the relative activity of caspase-3 in lysates of all cell lines as a function of PAC-1 exposure duration. We expected that longer incubation times with PAC-1 would allow for greater amounts of sequestered procaspase-3 to be autocatalytically activated to caspase-3. Indeed, there was good association between caspase-3 activity elevations and time-dependent cytotoxicity for 10 μM PAC-1 (Figures 3a, c, e and Figure 4a-c). Incubation times with PAC-1 for 48 hours produced the greatest percentage of apoptotic cells (Figures 3b,d, and f), which corresponded with the relative greatest cell lysate caspase-3 activity in all three B-cell lymphoma lines evaluated (Figure 4a-c). Similar trends between caspase-3 activation and induced cytotoxicity were also observed with 20 μM PAC-1 (data not shown). Interestingly, incubation times of ≤ 4 hours with PAC-1 (10 or 20 μM), failed to significantly increase cell lysate caspase-3 activity above vehicle-treated control cells, suggesting that a minimum threshold exists for how long cells must be exposed to PAC-1 before activating sufficient quantities of procaspase-3 necessary to irreversibly trigger apoptosis.

Pharmacokinetics of PAC-1 in healthy dogs

Dogs are frequently used in preclinical toxicity studies for investigating experimental therapeutics including anticancer agents. Serving as a large mammalian experimental system, dogs more closely mimic the body size, physiology, and metabolism of humans in comparison to rodents. As such, we sought to characterize the IV and oral pharmacokinetic

profiles of PAC-1 in six healthy research dogs through the conductance of a crossover design. Following single-dose, bolus IV PAC-1 at a dosage of 1.0 mg/kg, the average peak plasma concentration achieved immediately following the completion of drug infusion was 2.8 ± 0.6 μM (Figure 5a), with the mean terminal elimination half-life of 3.12 ± 0.67 (SD) hours (Table 1). Orally administered PAC-1 dosed at 1.0 mg/kg produced an average peak plasma concentration of 0.5 ± 0.1 μM 45 minutes following ingestion (Figure 5b), with an elimination half-life of 2.08 ± 0.26 (SD) hours. The oral bioavailability of PAC-1 was relatively low and highly variable, averaging 17.8 ± 9.5% (Table 2).

Pharmacokinetic-derived dosing regimen and toxicity assessment of constant rate infusion PAC-1

Based upon our *in vitro* conditions, the ability of PAC-1 to activate procaspase-3 to caspase-3 appeared both time- and dose-dependent. Minimal conditions identified most conducive for the induction of apoptosis in the cell lines evaluated were 1) exposure durations ≥ 24 hours and 2) PAC-1 concentrations ≥ 10 μM. With the known pharmacokinetics of PAC-1 in dogs characterized by our study, we were next able to pharmacokinetically derive a continuous rate infusion protocol predicted to achieve and maintain plasma concentrations of PAC-1 ≥ 10 μM for ≥ 24 hours, which correlates with similar *in vitro* conditions that proved cytotoxic to lymphoma cells in culture.

Using four of the same research dogs that were utilized to generate the pharmacokinetic profile of IV PAC-1; we were able to “personalize” their IV CRI protocol based upon their individualized volumes of distribution, systemic clearance, elimination half-life, and body weights. The IV CRI protocol tested in our investigation included a 10-minute loading dose (LD), followed by a CRI maintenance dosage (MD) administered for 48 hours. The “personalized” intravenous CRI dosages were calculated to be the following: Dog A, LD 6.4 mg/kg and MD 2.3 mg/kg/hour; Dog B, LD 4.5 mg/kg and MD 1.7 mg/kg/hour; Dog C, LD 6.9 mg/kg and MD 2.7 mg/kg/hour; and Dog D, LD 5.5 mg/kg and MD 2.4 mg/kg/hour. Collectively, the average LD and MD was calculated to be 5.8 mg/kg and 2.3 mg/kg/hour, respectively. Using this pharmacokinetically-derived dosing protocol, plasma concentrations of PAC-1 after 6 hours of infusion were 10.7 ± 2.0 μM, and remained equal to or greater than this concentration for approximately 36 hours (Figure 6). PAC-1 concentrations appeared to plateau off following completion of the first 24 hours of the CRI, with plasma concentrations ~18 μM.

In addition to characterizing the feasibility for instituting a pharmacokinetically-derived dosing regimen with PAC-1, in the same 4 dogs we determined the associated hematologic, non-hematologic, and gastrointestinal toxicity associated with a 48-hour exposure to micromolar concentrations of PAC-1. Following PAC-1 48-hour CRI, dogs were re-evaluated weekly for 4 consecutive weeks. Weekly serial blood tests and physical examinations documented the absence of any clinically meaningful hematologic and non-hematologic toxicity (Table 3). In addition, no clinically overt gastrointestinal toxicity was reported by animal care givers throughout the 4 week duration of monitoring.

DISCUSSION AND CONCLUSION

Procaspase activating compounds, such as PAC-1, hold promise as novel therapeutics for the treatment of cancer. However, prior to their clinical translation to human patients, the characterization of the apoptotic properties and pharmacokinetics of PAC-1 in appropriate model systems is necessary to streamline the drug discovery pathway. In this investigation, we demonstrate that PAC-1 induced apoptosis in a panel of B-cell lymphoma lines in a time- and dose-dependent manner. *In vitro* conditions conducive for PAC-1 to cause programmed cell death were exposure durations ≥ 24 hours with concurrent concentrations ≥ 10 μM.

Importantly, pharmacokinetic studies with PAC-1 conducted in healthy research dogs demonstrated the feasibility of achieving and maintaining concentrations of PAC-1 predicted to correlate with *in vitro* cytotoxic conditions. Not only were we able to successfully institute a pharmacokinetically-derived dosing protocol, but also this treatment regimen was well-tolerated in a large mammalian model which closely mimics the body size, physiology, and metabolism of humans. As such, it is likely that our data derived from dogs will be informative for expediting the further development of procaspase-3 activating compounds, such as PAC-1, for translational applications in people with cancer.

One interesting aspect of our study was the identification of one lymphoma cell line, GL-1, which appeared less sensitive to the apoptotic effects of PAC-1. Procaspase-3 concentrations were detectable in this cell line (MFI ratio of 1.7) and were similar to those in the human B-cell CA46 lymphoma line (MFI ratio of 1.8) (Figure 1). Despite the similarities in basal procaspase-3 concentrations, PAC-1 was considerably more effective for inducing apoptosis in CA46 cells (≥ 50% apoptosis with 48 hour and 10 μM conditions) in comparison with GL-1 cells (~ 25% apoptosis with 48 hour and 10 μM conditions) (Figure 3). One potential explanation for this observed difference in cytotoxicity between CA46 and GL-1 cells irrespective of basal procaspase-3 concentrations could be differences in two additional protein families which directly regulate caspase activity, specifically inhibitors of apoptotic proteins (IAPs) and second mitochondria-derived activator of caspases (Smac) (Hay et al., 1995; Deveraux et al., 1999; Lin et al., 2000; Kasof and Gomes, 2001; Suzuki et al., 2001). Differences in basal IAPs or Smac concentrations among differing cell lines could directly influence the apoptotic affects of PAC-1 by regulating overall caspase-3 activities.

In our investigation, we specifically included canine B-cell lymphoma lines for *in vitro* studies and normal research dogs for all pharmacokinetic and toxicity *in vivo* studies in an effort to expedite the translational development of PAC-1 or other procaspase activators for human cancer patients. Spontaneously-arising cancers in dogs share many similarities with people including histologic appearance, tumor genetics, molecular targets, biologic and clinical behavior, and response to therapy (Khanna et al., 2006). The biologic and clinical progression of large B-cell lymphoma in dogs recapitulates common variants of Non-Hodgkin's lymphoma in people, specifically diffuse large B-cell variants (Hahn et al., 1994; Vail and MacEwen, 2000). Similarly, dogs with lymphoma and humans diagnosed with Non-Hodgkin's lymphoma respond favorably to the same chemotherapeutic agents including cyclophosphamide, doxorubicin, vincristine, and prednisone (Coiffier, 2006; Rassnick et al., 2007), suggesting that the discovery of novel and effective agents in dogs with lymphoma would have high likelihood of exerting similar anticancer effects in humans (Paoloni and Khanna, 2008).

Using dogs greater than 30 kilograms in weight, we were able to demonstrate the feasibility and safety of PAC-1 IV therapy in an experimental system which more closely approximates the anatomic size, physiology, and metabolism of human beings when compared to conventional rodent models. As such, this investigation provides pertinent and valuable information for future plausible PAC-1 dosing strategies which may be well-tolerated and effective in human cancer patients.

In conclusion, PAC-1 is a small molecule that preferentially activates procaspase-3 to caspase-3, and induces apoptotic death in canine and human B-cell lymphoma lines. PAC-1 can be safely administered to research dogs and be consistently maintained at concentrations for prolonged periods of time which are predicted to exert anticancer effects.

Glossary

CRI	constant rate infusion
PAC-1	procaspase-3 activating compound 1

Acknowledgments

We thank Mrs. Holly Pondenis and Mr. Ian Sprandel for helping with *in vitro* laboratory experiments, and Mrs. Rebecca Kamerer and Nancy George for aiding canine pharmacokinetic experiments.

This work is supported in part by the Office of the Vice President for Technology and Economic Development at the University of Illinois, and the National Institutes of Health (R01-CA120439, PJH). QPP was supported by a Chemistry-Biology Interface Training Grant from the NIH (Ruth L. Kirschstein National Research Service Award 1 T32 GM070421) and by a predoctoral fellowship from the Medicinal Chemistry Division of the American Chemical Society. DCW was partially supported by Ruth L. Kirschstein National Research Service Award F31-CA130138-01S1.

REFERENCES

Arnold R, Brenner D, Becker M, Frey CR, Krammer PH. How T lymphocytes switch between life and death. Eur J Immunol. 2006; 36:1654–1658. [PubMed: 16791883]

Coiffier B. Treatment of non-Hodgkin's lymphoma: a look over the past decade. Clin Lymphoma Myeloma. 2006; 7 Suppl 1:S7–S13. [PubMed: 17101073]

Deveraux QL, Leo E, Stennicke HR, Welsh K, Salvesen GS, Reed JC. Cleavage of human inhibitor of apoptosis protein XIAP results in fragments with distinct specificities for caspases. Embo J. 1999; 18:5242–5251. [PubMed: 10508158]

Downward J. PI 3-kinase, Akt and cell survival. Semin Cell Dev Biol. 2004; 15:177–182. [PubMed: 15209377]

Dukers DF, Oudejans JJ, Vos W, ten Berge RL, Meijer CJ. Apoptosis in B-cell lymphomas and reactive lymphoid tissues always involves activation of caspase 3 as determined by a new in situ detection method. J Pathol. 2002; 196:307–315. [PubMed: 11857494]

Fink D, Schlagbauer-Wadl H, Selzer E, Lucas T, Wolff K, Pehamberger H, Eichler HG, Jansen B. Elevated procaspase levels in human melanoma. Melanoma Res. 2001; 11:385–393. [PubMed: 11479427]

Fisher RI, Gaynor ER, Dahlberg S, Oken MM, Grogan TM, Mize EM, Glick JH, Coltman CA Jr, Miller TP. Comparison of a standard regimen (CHOP) with three intensive chemotherapy regimens for advanced non-Hodgkin's lymphoma. N Engl J Med. 1993; 328:1002–1006. [PubMed: 7680764]

Gibaldi, M.; Perrier, D. Pharmacokinetics. New York: Marcel Dekker; 1975. p. 281

Gibaldi, M.; Perrier, D. Pharmacokinetics. 2nd edn. New York: Marcel Dekker; 1982. p. 409-447.

Gurumurthy S, Vasudevan KM, Rangnekar VM. Regulation of apoptosis in prostate cancer. Cancer Metastasis Rev. 2001; 20:225–243. [PubMed: 12085964]

Hahn KA, Bravo L, Adams WH, Frazier DL. Naturally occurring tumors in dogs as comparative models for cancer therapy research. In Vivo. 1994; 8:133–143. [PubMed: 8054503]

Hanahan D, Weinberg RA. The hallmarks of cancer. Cell. 2000; 100:57–70. [PubMed: 10647931]

Hay BA, Wassarman DA, Rubin GM. Drosophila homologs of baculovirus inhibitor of apoptosis proteins function to block cell death. Cell. 1995; 83:1253–1262. [PubMed: 8548811]

Hildeman DA, Zhu Y, Mitchell TC, Kappler J, Marrack P. Molecular mechanisms of activated T cell death in vivo. Curr Opin Immunol. 2002; 14:354–359. [PubMed: 11973134]

Izban KF, Wrone-Smith T, Hsi ED, Schnitzer B, Quevedo ME, Alkan S. Characterization of the interleukin-1beta-converting enzyme/ced-3-family protease, caspase-3/CPP32, in Hodgkin's disease: lack of caspase-3 expression in nodular lymphocyte predominance Hodgkin's disease. Am J Pathol. 1999; 154:1439–1447. [PubMed: 10329597]

Kasof GM, Gomes BC. Livin, a novel inhibitor of apoptosis protein family member. J Biol Chem. 2001; 276:3238–3246. [PubMed: 11024045]

Khanna C, Lindblad-Toh K, Vail D, London C, Bergman P, Barber L, Breen M, Kitchell B, McNeil E, Modiano JF, Niemi S, Comstock KE, Ostrander E, Westmoreland S, Withrow S. The dog as a cancer model. Nat Biotechnol. 2006; 24:1065–1066. [PubMed: 16964204]

Krepela E, Prochazka J, Liul X, Fiala P, Kinkor Z. Increased expression of Apaf-1 and procaspase-3 and the functionality of intrinsic apoptosis apparatus in non-small cell lung carcinoma. Biol Chem. 2004; 385:153–168. [PubMed: 15101558]

Li J, Yuan J. Caspases in apoptosis and beyond. Oncogene. 2008; 27:6194–6206. [PubMed: 18931687]

Lin JH, Deng G, Huang Q, Morser J. KIAP, a novel member of the inhibitor of apoptosis protein family. Biochem Biophys Res Commun. 2000; 279:820–831. [PubMed: 11162435]

Martinez MN. Noncompartmental methods of drug characterization: statistical moment theory. J Am Vet Med Assoc. 1998a; 213:974–980. [PubMed: 9776992]

Martinez MN. Use of pharmacokinetics in veterinary medicine. Article. II: Volume, clearance, and half-life. J Am Vet Med Assoc. 1998b; 213:1122–1127. [PubMed: 9787378]

Medema JP, Borst J. T cell signaling: a decision of life and death. Hum Immunol. 1999; 60:403–411. [PubMed: 10447398]

Mori C, Nakamura N, Kimura S, Irie H, Takigawa T, Shiota K. Programmed cell death in the interdigital tissue of the fetal mouse limb is apoptosis with DNA fragmentation. Anat Rec. 1995; 242:103–110. [PubMed: 7604973]

Muris JJ, Cillessen SA, Vos W, van Houdt IS, Kummer JA, van Krieken JH, Jiwa NM, Jansen PM, Kluin-Nelemans HC, Ossenkoppele GJ, Gundy C, Meijer CJ, Oudejans JJ. Immunohistochemical profiling of caspase signaling pathways predicts clinical response to chemotherapy in primary nodal diffuse large B-cell lymphomas. Blood. 2005; 105:2916–2923. [PubMed: 15576477]

Nakagawara A, Nakamura Y, Ikeda H, Hiwasa T, Kuida K, Su MS, Zhao H, Cnaan A, Sakiyama S. High levels of expression and nuclear localization of interleukin-1 beta converting enzyme (ICE) and CPP32 in favorable human neuroblastomas. Cancer Res. 1997; 57:4578–4584. [PubMed: 9377572]

O'Donovan N, Crown J, Stunell H, Hill AD, McDermott E, O'Higgins N, Duffy MJ. Caspase 3 in breast cancer. Clin Cancer Res. 2003; 9:738–742. [PubMed: 12576443]

Paoloni M, Khanna C. Translation of new cancer treatments from pet dogs to humans. Nat Rev Cancer. 2008; 8:147–156. [PubMed: 18202698]

Peterson QP, Goode DR, West DC, Ramsey KN, Lee JJ, Hergenrother PJ. PAC-1 activates procaspase-3 in vitro through relief of zinc-mediated inhibition. J Mol Biol. 2009a; 388:144–158. [PubMed: 19281821]

Peterson QP, Hsu DC, Goode DR, Novotny CJ, Totten RK, Hergenrother PJ. Procaspase-3 activation as an anti-cancer strategy: structure-activity relationship of procaspase-activating compound 1 (PAC-1) and its cellular co-localization with caspase-3. J Med Chem. 2009b; 52:5721–5731. [PubMed: 19708658]

Pop C, Salvesen GS. Human caspases: activation, specificity, and regulation. J Biol Chem. 2009; 284:21777–21781. [PubMed: 19473994]

Putt KS, Chen GW, Pearson JM, Sandhorst JS, Hoagland MS, Kwon JT, Hwang SK, Jin H, Churchwell MI, Cho MH, Doerge DR, Helferich WG, Hergenrother PJ. Small-molecule activation of procaspase-3 to caspase-3 as a personalized anticancer strategy. Nat Chem Biol. 2006; 2:543–550. [PubMed: 16936720]

Rassnick KM, McEntee MC, Erb HN, Burke BP, Balkman CE, Flory AB, Kiselow MA, Autio K, Gieger TL. Comparison of 3 protocols for treatment after induction of remission in dogs with lymphoma. J Vet Intern Med. 2007; 21:1364–1373. [PubMed: 18196748]

Shargel, L.; Yu, ABC. Applied biopharmaceuticals and pharmacokinetics. 3rd edn. Norwalk: Appleton and Lange Publishers; 1993.

Suzuki Y, Nakabayashi Y, Nakata K, Reed JC, Takahashi R. X-linked inhibitor of apoptosis protein (XIAP) inhibits caspase-3 and -7 in distinct modes. J Biol Chem. 2001; 276:27058–27063. [PubMed: 11359776]

Takanosu M, Amasaki H, Iwama Y, Ogawa M, Hibi S, Suzuki K. Epithelial cell proliferation and apoptosis in the developing murine palatal rugae. Anat Histol Embryol. 2002; 31:9–14. [PubMed: 11841352]

Vail DM, MacEwen EG. Spontaneously occurring tumors of companion animals as models for human cancer. Cancer Invest. 2000; 18:781–792. [PubMed: 11107448]

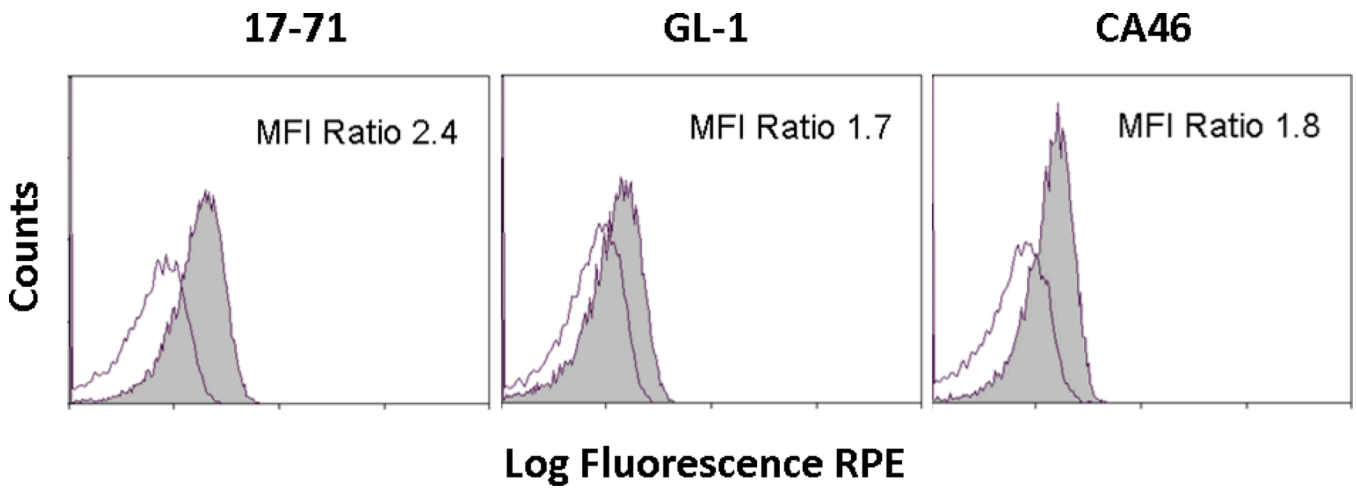

Figure 1.

Demonstration of procaspase-3 levels in immortalized cell lines. The relative expression levels of procaspase-3 in 17-71 (left), GL-1 (middle), and CA46 (right) B-cell lymphoma lines were determined. Staining for procaspase-3 is represented by shaded grey line and non-specific staining by an isotype control antibody is marked with open black line. Mean fluorescent intensity (MFI) ratios expressed as the fraction (procaspase-3 MFI)/(isotype control MFI) was used to compare relative differences or similarities in basal procaspase-3 levels among cell lines.

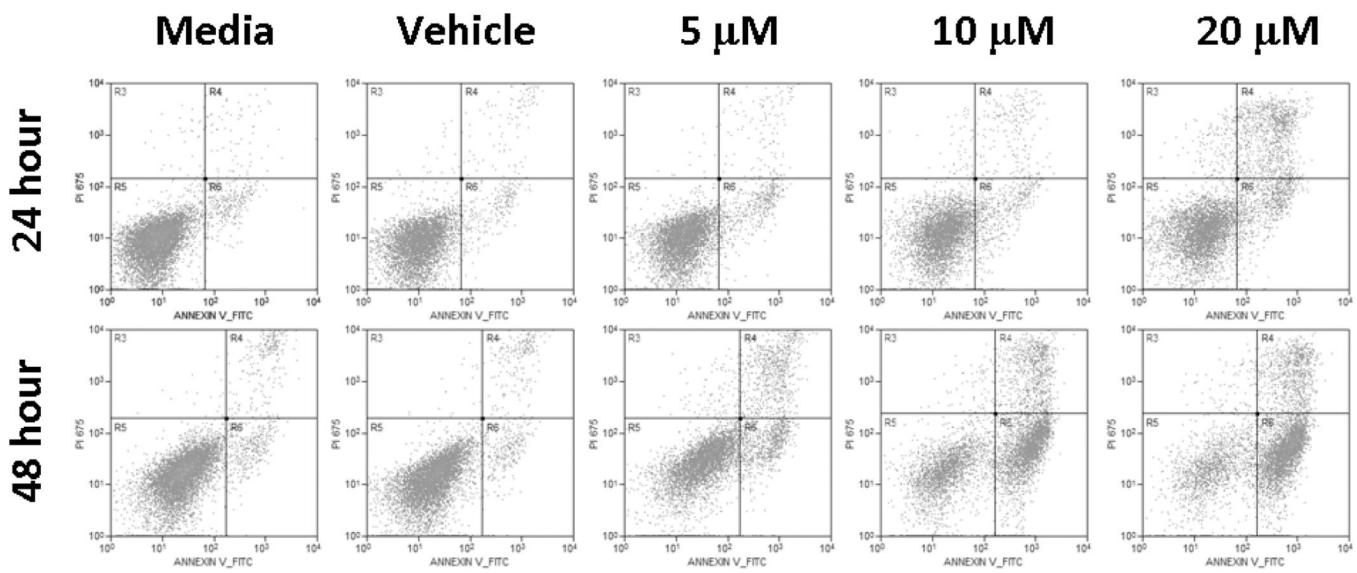

Figure 2.

PAC-1 induces apoptosis. The selective ability of PAC-1 to induce cell death through apoptosis, not necrosis, is demonstrated in the 17-71 cell line. Maximal apoptosis is induced with 48 hour exposure durations and 20 µM concentrations, with approximately 70% of cells staining only for Annexin-V-FITC (right lower quadrant), an early apoptotic marker.

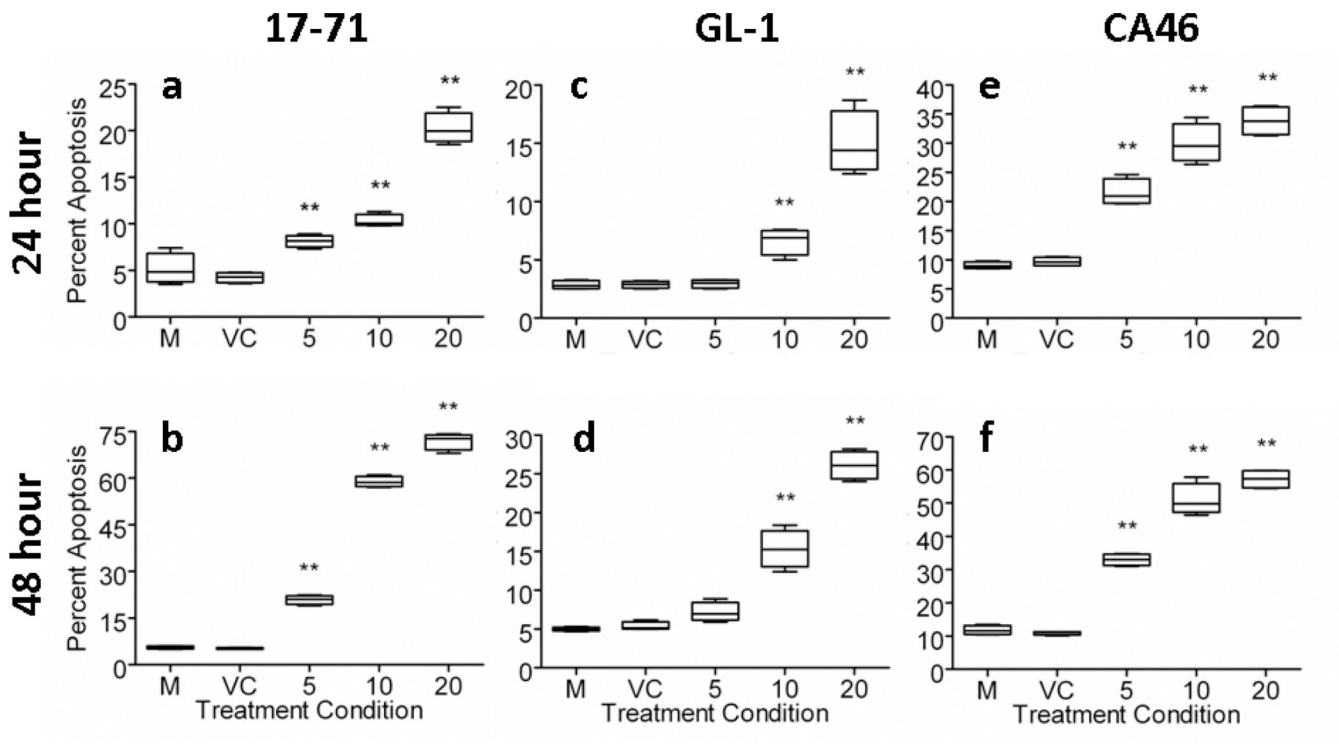

Figure 3.

PAC-1 exerts time- and dose-dependent apoptotic effects. The ability of PAC-1 to induce apoptosis is influenced by exposure durations and concentrations. Treatment conditions which resulted in significant increases in the percentage of apoptotic cells compared to control cells incubated with media (M) alone represented by double asterisks with $p < 0.01$. 17-71 (a, b) and CA46 (e, f) cell lines are more sensitive to the apoptotic effects of PAC-1 in comparison with the GL-1 (c, d) cell line. VC = Vehicle control; all PAC-1 concentrations are in μM. Error bars represent standard deviation, n = 5.

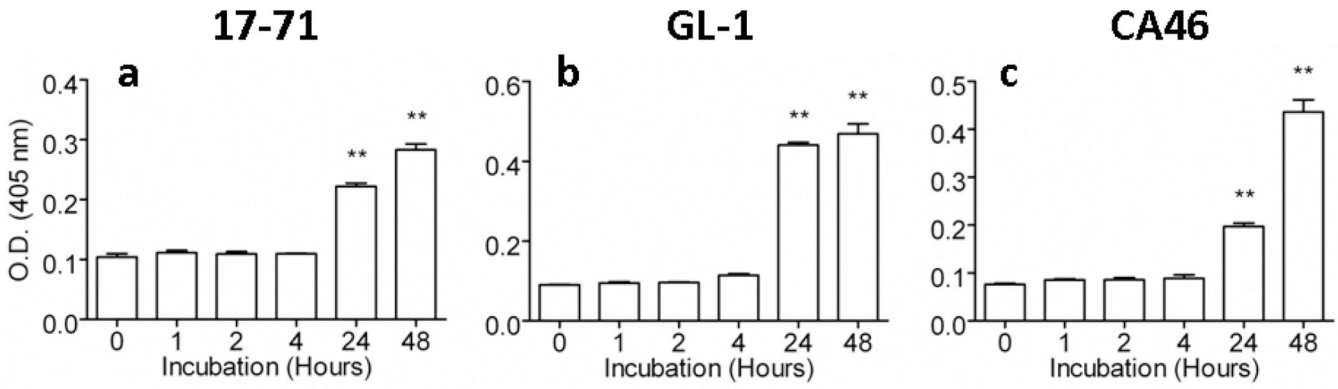

Figure 4.

Observed apoptosis correlates with caspase-3 activity in cell lysate. Time- and dose-dependent apoptotic death induced by PAC-1 is correlated with increases in caspase-3 activity. A 10 μM concentration of PAC-1 significantly increases caspase-3 activity (as measured by mean optical densities) in 17-71 (a), GL-1 (b), and CA46 (c) cell lines, but requires greater than 4 hours of drug exposure. At 10 μM PAC-1 concentrations, treatment conditions which induce significant increases in caspase-3 activities above vehicle control treated cells (Hour 0) is represented by double asterisk, $p < 0.01$. Error bars represent standard deviation, $n = 4$. Similar results were observed for PAC-1 concentrations of 20 μM (data not shown).

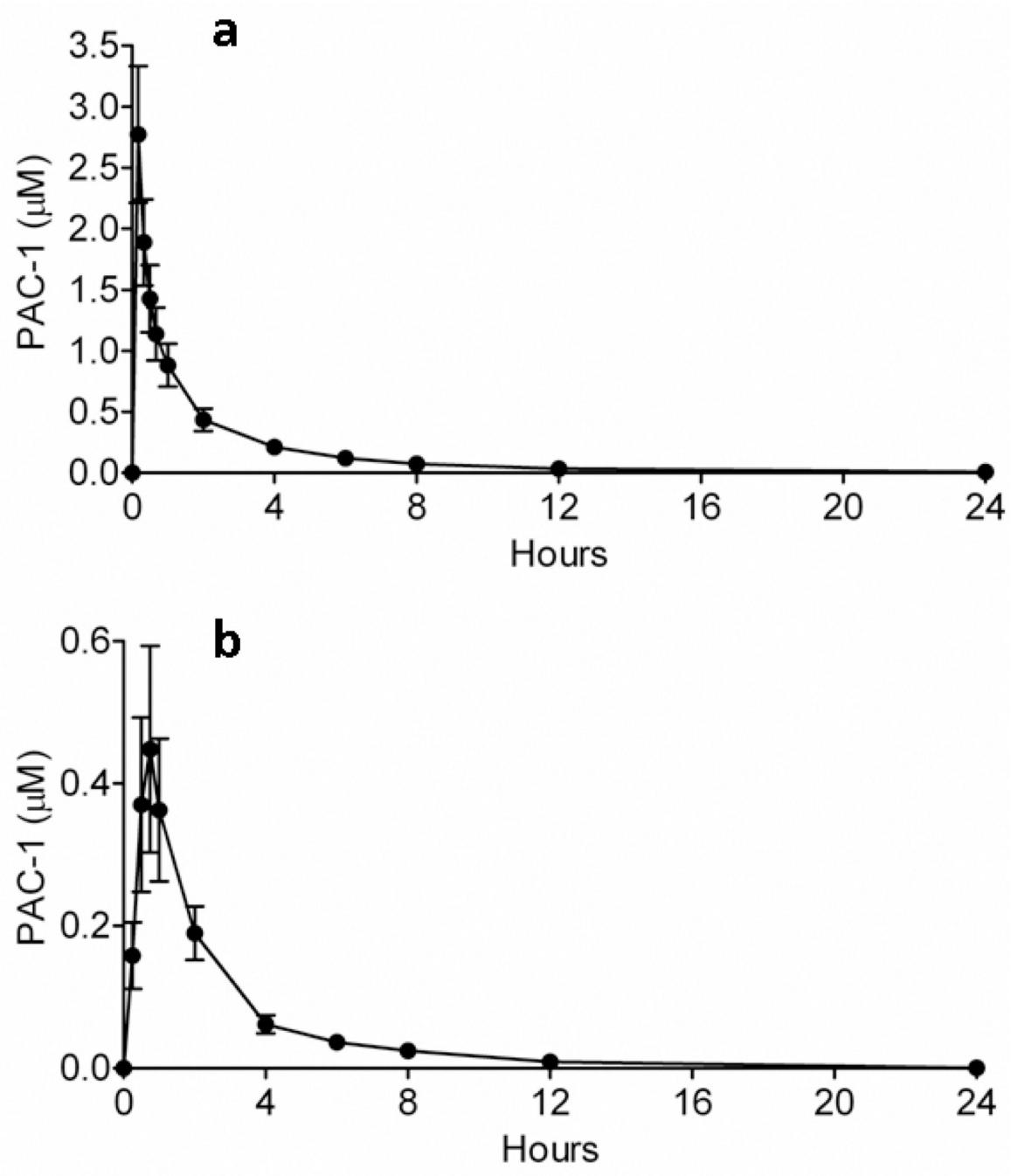

Figure 5.
Pharmacokinetics of PAC-1 in healthy dogs. The pharmacokinetic profiles of (a) intravenous and (b) oral PAC-1 were characterized in 6 healthy dogs using a crossover design. Intravenous PAC-1 produces higher and more consistent peak plasma concentrations in comparison with orally administered PAC-1. Error bars represent standard deviation, n = 6.

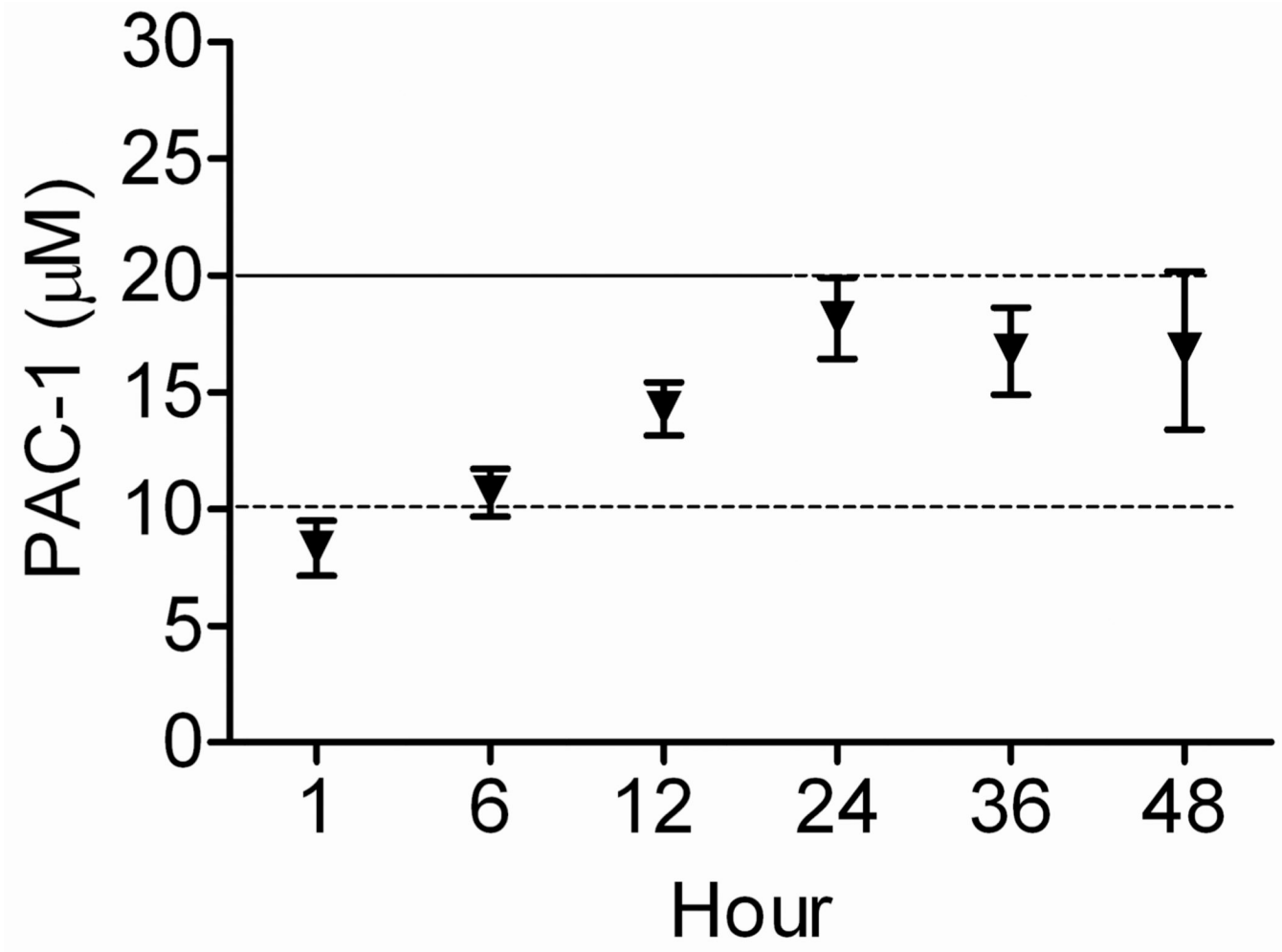

Figure 6.

Continuous rate infusion of PAC-1. A pharmacokinetically-derived dosing regimen, designed to achieve and maintain steady state plasma concentrations of PAC-1 predicted to exert time- and dose-dependent cytotoxic effects, was evaluated in healthy dogs. The achievement of predicted PAC-1 cytotoxic concentrations ≥ 10 μM, as well as durations of exposure ≥ 24 hours was technically feasible and biologically well-tolerated by all dogs. Error bars represent standard deviation, n = 4.

Table 1

Pharmacokinetic parameters of PAC-1 following single 1 mg/kg IV injection in dogs

Dog	**A**	**B**	**C**	**D**	**E**	**F**	**Mean ± SD**
Weight (kg)	37.1	31.3	27.7	30.8	33.3	31.1	31.9 ± 3.1
A (ng/ml)	1065	2598	908	2199	1119	1014	1483.8 ± 723.0
B (ng/ml)	288	584	138	176	154	154	249.0 ± 172.9
$t_{1/2}\ \alpha$ (hr)	0.392	0.121	0.636	0.273	0.611	0.412	0.408 ± 0.197
$t_{1/2}\ \beta$ (hr)	2.71	2.24	3.20	3.08	3.24	4.26	3.12 ± 0.67
Cl_s (ml/kg/hr)	578	428	603	608	585	646	574.7 ± 75.7
Vd_c (L/kg)	0.739	0.314	0.957	0.421	0.786	0.856	0.678 ± 0.254
Vd_β (L/kg)	2.260	1.380	3.145	2.699	2.736	3.968	2.698 ± 0.865
Vd_{ss} (L/kg)	1.587	1.127	1.715	1.405	1.454	2.574	1.643 ± 0.497
$AUC_{0\text{-}inf}$ (ngxhr/ml)	1730	2339	1468	1645	1709	1549	1740 ± 309.6
$AUMC_{0\text{-}inf}$ (ngxhrxhr/ml)	4751	6167	3693	3802	4247	6174	4805 ± 1211
R^2	0.99	0.99	0.99	0.99	0.99	0.99	0.99 ± 0

Table 2

Pharmacokinetic parameters of PAC-1 following single 1 mg/kg oral administration in dogs

Dog	**A**	**B**	**C**	**D**	**E**	**F**	**Mean ± SD**
Weight (kg)	37.1	31.3	27.7	30.8	33.3	31.1	31.9 ± 3.1
F (%)	16	17	8	31	8	27	17.8 ± 9.5
$t_{1/2}$ K_{10} (h)	2.02	1.83	1.86	2.40	1.97	2.42	2.08 ± 0.26
$t_{1/2}$ K_{01} (h)	0.36	0.12	0.28	0.32	0.10	0.28	0.24 ± 0.11
AUC $_{o\text{-}inf.}$ (ng/ml/h)	271	408	117	508	145	414	310.5 ± 158.5
Oral clearance (L/h)	137	77	236	61	230	75	136 ± 79.6
T_{max} (h)	1.09	0.51	0.90	1.07	0.45	0.99	0.84 ± 0.28
C_{max} (ng/ml)	63.9	127	31	108	43	89	77.0 ± 37.5
R^2	0.94	0.87	0.94	0.87	0.98	0.82	0.9 ± 0.06

Table 3

Hematologic and Non-hematologic tolerability of 48-hour PAC-1 CRI

Parameter	Reference	Day 0	Day 7	Day 14	Day 21
WBC	6–17.0×10^3	8.2 ± 1.5	7.0 ± 0.4	7.0 ± 0.4	8.4 ± 0.6
Neutrophil	3–11.5×10^3	5.4 ± 1.0	5.0 ± 0.5	4.3 ± 0.9	5.9 ± 0.3
Lymphocyte	1–4.8×10^3	1.9 ± 0.3	1.3 ± 0.2	1.9 ± 0.7	1.5 ± 0.2
Hematocrit	35–52%	53.0 ± 3.8	55.4 ± 1.3	49.3 ± 6.0	50.6 ± 3.4
Platelet	2–9×10^5	1.9 ± 0.4	1.8 ± 0.3	2.0 ± 0.4	2.2 ± 0.8
Creatinine	0.5–1.6 mg/dl	0.9 ± 0.2	1.0 ± 0.3	0.9 ± 0.1	1.0 ± 0.2
Calcium	7.9–11.5 mg/dl	10.3 ± 0.1	10.5 ± 0.3	10.2 ± 0.4	10.4 ± 0.4
Phosphorous	2.4–6.5 mg/dl	3.7 ± 0.4	2.9 ± 0.9	3.6 ± 0.3	3.4 ± 0.4
ALT	17–87 U/L	46.7 ± 34.1	57.0 ± 34.6	56.3 ± 46.7	49.7 ± 29.0